

## Use of P-1 model with the additional source term for numerical simulation of ultraviolet radiation in a photoreactor

Baoqing Deng<sup>\*,†</sup>, Daqiang Ge<sup>\*</sup>, Li Lu<sup>\*</sup>, Di Ge<sup>\*</sup>, Jiajia Li<sup>\*</sup>, Yuan Guo<sup>\*</sup>, and Chang Nyung Kim<sup>\*\*,†</sup>

<sup>\*</sup>Department of Environmental Science and Engineering, University of Shanghai for Science and Technology, Shanghai 200093, P. R. China

<sup>\*\*</sup>College of Engineering, Kyung Hee University, Yongin 446-701, Korea

(Received 4 May 2013 • accepted 24 February 2014)

**Abstract**—Radiation distribution in a photoreactor with multiple mediums is solved by the P-1 model. The UV lamp is included in the computational domain. An additional source term method is presented to describe the generation of UV light, which can avoid the use of analytical lamp emission model at the lamp surface. The boundary condition for incident radiation at the semi-transparent wall between adjacent mediums has been derived to link the P-1 equations in adjacent mediums, which enables the present model to adapt to the photoreactor with complicated structure. The predicted incident radiation agrees well with the experimental data in literature. The effects of absorption coefficient, scattering coefficient and phase function of lamp plasma on the radiation distribution are discussed in detail.

Keywords: P-1 Model, UV Reactor, Radiation Distribution, Multiple Mediums

### INTRODUCTION

It has been demonstrated that ultraviolet (UV) irradiation is an effective way for the inactivation of viruses and bacteria. Compared to the conventional chlorine disinfection units, UV irradiation is broadly effective on waterborne pathogens, bacteria and viruses, and it does not produce disinfection by-product [1]. To optimize the configuration of UV photoreactors, appropriate mathematical models are required, which should integrate the velocity field, the radiation field and the microorganism inactivation. In the last two decades, the remarkable development of computational fluid dynamics has enabled the prediction of velocity field to be accurate. Another important factor is the radiation field, which offers energy for the inactivation of bacteria. However, a solution of the radiation field is still a challenging task.

Many scholars have developed analytical light emission models to predict the radiation field in a photoreactor based on some theoretical assumptions. The commonly used analytical light emission models can be classified into three categories: (1) the point source model; (2) the line source model; (3) the extensive source model. The point source models include the multiple point source summation model [2,3] and the multiple segment source summation model [4,5], which take the lamp as a finite number of equally spaced point sources along the axis of the lamp and as a series of differential cylindrical segments, respectively. The line source models consist of the line source spherical emission model [6] and the line source with diffused emission model [7], which considers the lamp as a line-emitting radiation isotropically in all directions and emitting radiation diffusely following cosine law, respectively. The extensive source model considers the lamp to be a cylinder, in which the radiation is emitted

uniformly in three-dimensional space [8-10]. Compared to the point source model and the line source model, the extensive source model does not impose any simplification on the geometry of the lamp. The common feature of these models is that their mathematical expressions are simple and easy to compute. Yang et al. [11] evaluated the performance of analytical light emission models in an annular photoreactor. They concluded that these models performed well.

The aforementioned analytical lamp emission models require a simple and regular structure of the photoreactor and a single medium in the photoreactor. For complicated structures of the photoreactor, these analytical lamp emission models may reduce the precision. Moreover, the scattering effect is not taken into account in analytical lamp emission models [12]. However, scattering may cause a reduction in the absorbed power and thus in the conversion of the photochemical reaction [13,14]. Therefore, direct solution of the radiative transfer equation (RTE) becomes an alternative. During the past few decades, several numerical methods have been proposed to solve the RTE in complicated geometry. Several researchers used the finite volume method to solve the radiation distribution in the photoreactor [9,15,16]. Pareek and Adesina [17] used a conservative variant discrete ordinate (DO) method to investigate the effect of wall reflectivity and phase function on the distribution of light radiation in a slurry photoreactor. DO method produces relatively accurate results because it does not involve any simplified assumption than other discretization of pertinent partial differential equations. However, the RTE is only integrated over the control volume in the DO method, so it does not conserve the radiant energy at the surfaces of complex geometries especially for the anisotropic scattering. Yu et al. [18] developed the P-1 model to predict the light intensity in the photoreactor. A drawback is that these numerical models require the result of analytical lamp emission model as the boundary condition at the lamp surface because the lamp region is excluded from the computational domain.

This paper aims to predict the radiation distribution in a photore-

<sup>†</sup>To whom correspondence should be addressed.  
E-mail: bqdeng@usst.edu.cn, cnkim@khu.ac.kr  
Copyright by The Korean Institute of Chemical Engineers.

actor with multiple mediums. The generation of UV light is included into the mathematical model to avoid the use of analytical lamp emission model. The boundary condition at the interface between adjacent mediums is developed. Experimental data from Duran et al. [19] is used to validate the present model.

## MODEL DEVELOPMENT

### 1. P-1 Model

A UV lamp is usually positioned inside a photoreactor. UV light is emitted from the UV lamp and transfers inside the inner space of the photoreactor. Radiation intensity  $I$  ( $\text{W}\cdot\text{m}^{-2}\cdot\text{sr}^{-1}$ ) is used to describe radiation transfer. However, the incident radiation  $G$  ( $\text{W}\cdot\text{m}^{-2}$ ) instead of the radiation intensity takes effect in the photoreaction. The incident radiation  $G$  is defined as follows

$$G(\vec{r}) = \int_{4\pi} I(\vec{r}, \vec{\xi}) d\Omega \quad (1)$$

where  $\Omega$  is solid angle (sr).

There are two methods to obtain the incident radiation  $G$ . One way is to solve the radiative transfer equation such as using DO method and then perform the integration using Eq. (1). When using DO method to solve Eq. (1), an enough fine spatial and angular discretization is required to ensure the smoothness of the incident radiation, which means a large computational effort. The other one is to construct the governing equation of the incident radiation  $G$  and solve the incident radiation directly, which can save computational effort. The governing equation of the incident radiation  $G$  can be written as [18]

$$\nabla \cdot (\Gamma_G \nabla G) - aG = S \quad (2)$$

with

$$\Gamma_G = \frac{1}{3(a + \sigma_s) - C\sigma_s} \quad (3)$$

where  $\Gamma_G$  is the diffusion coefficient of the incident radiation (m),  $a$  the absorption coefficient ( $\text{m}^{-1}$ ),  $\sigma_s$  the scattering coefficient ( $\text{m}^{-1}$ ),  $C$  the linear-anisotropic phase function coefficient and  $S$  a user-defined radiation source ( $\text{W}\cdot\text{m}^{-3}$ ).

Eq. (2) is called the P-1 model.  $\Gamma_G$  stands for the rate of transport of incident radiation and is determined by the absorption coefficient, scattering coefficient and the phase function. The temperature-related source term has been omitted in Eq. (2) because temperature is not high in the photoreactor so that the spontaneous emission is seldom located in the range of ultraviolet range.

### 2. Boundary Conditions at Semi-transparent Walls

When including a UV lamp into a computational domain, multiple transparent mediums in UV reactor, such as lamp plasma, air, water, and quartz, must be taken into account in the calculation. However, Eq. (2) is derived for a single medium and cannot be directly used for a computational domain with multiple transparent mediums because it does not consider the transmitting of UV light at semi-transparent walls between adjacent mediums. Thus, boundary conditions at semi-transparent walls are required so as to link the P-1 equation in different mediums.

For semi-transparent walls inside UV reactor, as shown in Fig. 1, the rays coming from medium a into medium b are divided into

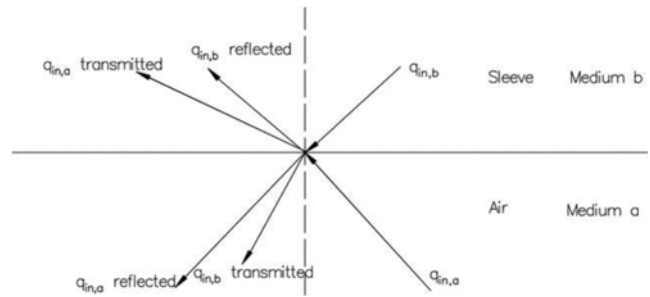


Fig. 1. Schematic representation of the semi-transparent wall.

the transmitted part and the reflected part and vice versa. Since medium a and medium b have different refractive indexes, absorption coefficients and scattering coefficients, the distribution of radiation intensity in medium a is different from that in medium b. It is assumed that diffuse reflection and diffuse refraction exist on both sides of the interface between medium a and medium b. By assuming that the outward normal vector  $\vec{n}$  pointing from medium b to medium a, the radiation intensity leaving the interface in medium b can be written as

$$I_{wb}(\vec{r}, \vec{\xi}) = \frac{\rho_{wb}}{\pi} \int_{\vec{n} \cdot \vec{\xi} > 0} I(\vec{r}, \vec{\xi}) \vec{n} \cdot \vec{\xi} d\Omega - \frac{\tau_{wa}}{\pi} \int_{\vec{n} \cdot \vec{\xi} > 0} I(\vec{r}, \vec{\xi}) \vec{n} \cdot \vec{\xi} d\Omega \quad (4)$$

The first term on the right-hand side of Eq. (4) stands for the reflected part of the light illuminated on the interface from the medium b. The second term on the right-hand side of Eq. (4) stands for the transmitted part of the light illuminated on the interface from the medium a. By applying Marshak's boundary condition,

$$\int_{2\pi} I_{wb}(r, s) \vec{n} \cdot \vec{\xi} d\Omega = \int_{2\pi} I(r, s) \vec{n} \cdot \vec{\xi} d\Omega \quad \vec{n} \cdot \vec{\xi} < 0 \quad (5)$$

we can obtain

$$-\Gamma_G \frac{\partial G}{\partial n} = G \frac{1 - \rho_{wb} - \tau_{wa}}{2(1 + \rho_{wb} - \tau_{wa})} \quad (6)$$

where  $\rho_{wb}$  is the reflectivity of the semi-transparent wall in the medium b, and  $\tau_{wa}$  is the transmissivity of the semi-transparent wall in the medium a. Eq. (6) requires two sets of reflectivity, transmissivity and diffusion coefficients  $\Gamma_G$ .

### 3. Radiation Source Modeling

In a UV reactor, UV light is emitted from a UV lamp. Fig. 2(a) shows a schematic of a UV reactor. The UV lamp must be consid-

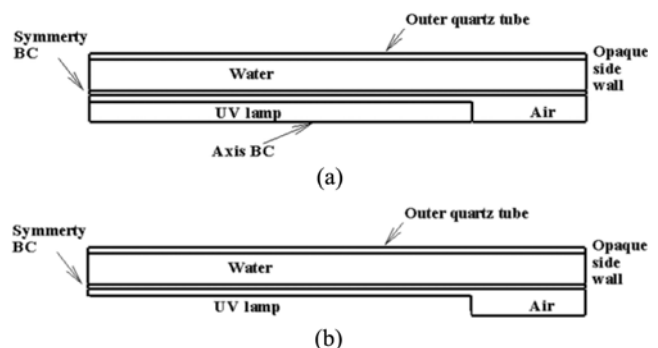


Fig. 2. 2D computational domain of the annular reactor.

ered in a mathematical model when simulating the incident radiation. The previous methodology excluded UV lamp from the computational domain, as shown in Fig. 2(b). Then, the results of analytical lamp emission models were adopted as the boundary conditions of DO model or P-1 model at the lamp surface [17,18,20]. When the lamp is viewed as a line emitting photons, the energy from outside radiation intensity at the lamp surface can be evaluated by

$$G|_{hw} = \frac{P}{4\pi rL} \left[ \arctan\left(\frac{z+\frac{1}{2}L}{r}\right) - \arctan\left(\frac{z-\frac{1}{2}L}{r}\right) \right] \quad (7)$$

where  $P_{Lamp}$  is the emission power of the UV lamp (W),  $L$  the length of the lamp,  $z$  the axial distance and  $r$  the radial distance where the origin is located in the lamp center. It should be pointed out that boundary conditions from analytical lamp emission models, i.e., Eq. (7), may be imprecise because of the complicated internal structure and the existence of multi-medium in a UV reactor.

In the present study, an additional source term method is developed to describe the generation of UV light. The treatment herein assumes:

- (1) The UV light is generated uniformly in the lamp region.
- (2) The medium, i.e., plasma, in the lamp region can absorb and scatter UV light.

Thus, the source term  $S$  in Eq. (2) can be defined as follows:

$$S = \begin{cases} P_{lamp}/V_{lamp} & \text{the lamp region} \\ 0 & \text{the other parts in the photoreactor} \end{cases} \quad (8)$$

where  $V_{Lamp}$  is the volume of the lamp ( $m^3$ ). The incident radiation at the lamp surface is computed by Eq. (2) itself instead of analytical lamp emission models, which overcomes the inconsistency between analytical lamp emission models and DO model or P-1 model.

## RESULTS AND DISCUSSION

### 1. Validation

The experimental data from Duran et al. [19] is used to validate the present model. As shown in Fig. 2(a), the tubes inside the reactor are made of quartz (inner tube: 23 mm OD/20 mm ID, outer tube: 50 mm OD/46 mm ID). A low-pressure Hg lamp (arc length=277 mm, tube diameter=15 mm, nominal UV output at 254 nm=5.7 W) is placed at the center of the reactor. The absorption coefficients are listed in Table 1, which is taken from Duran et al. [19]. A two-dimensional axisymmetric simulation is performed due to the symmetry of the annular reactor. The commercial CFD software Fluent is used to solve Eq. (2). To ensure grid independence, 240,000 grids are used in the calculation. The boundary conditions, the source terms and the diffusion coefficients are introduced into Fluent by UDF codes. The iterations are performed until the normalized residuals become less than  $10^{-7}$ .

Fig. 3 shows the computed incident radiation and the experimen-

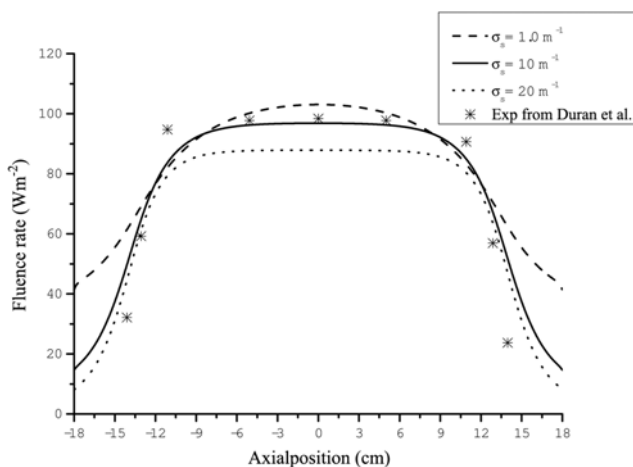


Fig. 3. The incident radiation at the outer wall of the photoreactor.

tal data at the reactor outer wall. Since the scattering coefficient of lamp plasma was not given in Duran et al. [19], three scattering coefficients were considered in the present study. The predicted incident radiation for the scattering coefficient of  $1\text{ m}^{-1}$  accords well with the experimental data in the central region, while there exists a big discrepancy in the region adjacent to the two ends. However, the predicted incident radiation for the scattering coefficient of  $10\text{ m}^{-1}$  and  $20\text{ m}^{-1}$  is in good agreement with the experimental data in the entire region. Although Eq. (7) can also obtain good results close to the experimental data, the implementation of (8) is relatively easier than that of Eq. (7).

### 2. Effect of Scattering Coefficient

As shown in Fig. 3, the scattering coefficient of lamp plasma has an influence on the incident radiation at the axial ends of the photoreactor. The effect of scattering coefficient of lamp plasma on incident radiation in the radial direction is depicted in Fig. 4. The predicted profiles with different scattering coefficients are similar in shape. Compared to Fig. 3, the magnitude of difference in the incident radiation for different scattering coefficient is small. It means that the scattering coefficient has more effect on the radial distribution than

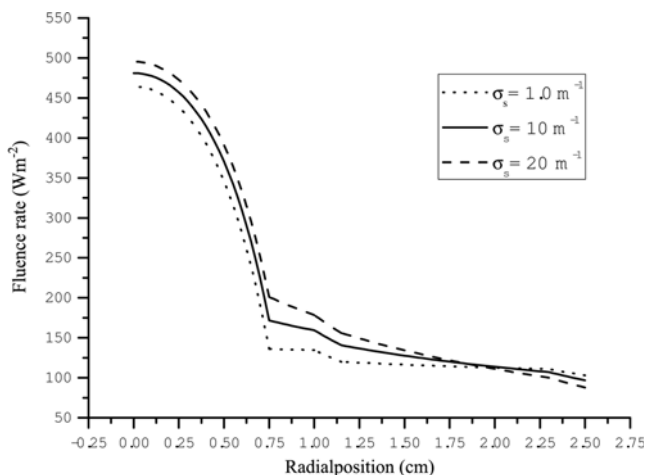


Fig. 4. The effect of scattering coefficient of the lamp plasma on incident radiation.

Table 1. Absorption coefficient (a) used in the simulations

Material	Lamp plasma	Air	Water	Quartz
$a\text{ (m}^{-1}\text{)}$	191	0	2.02	22

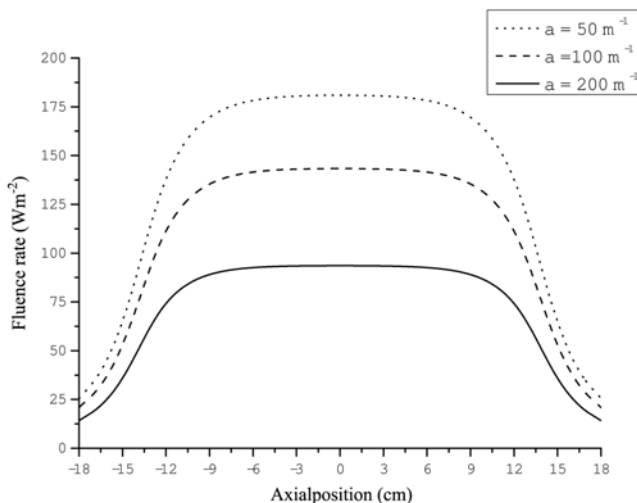


Fig. 5. The effect of absorption coefficient of the lamp plasma on incident radiation.

the axial distribution of incident radiation. All profiles are not smooth at the interface between the lamp and the air due to different optical properties, which leads to a big difference between the values of  $I_G$ . The incident radiation inside the lamp region is much higher. From the center of the lamp to the lamp envelope (0.0-0.75 cm), the incident radiation decreased sharply because of its high absorption coefficient ( $191 \text{ m}^{-1}$ ). Outside the lamp, the incident radiation curve becomes relatively flat.

### 3. Effect of Absorption Coefficient

Fig. 5 depicts the predicted incident radiation with different absorption coefficients of lamp plasma. The absorption coefficients in other parts of the computational domain are kept the same as before. The phase function coefficient  $C$  is zero. The scattering coefficient is taken to be  $10 \text{ m}^{-1}$ . The magnitudes of the incident radiation differ greatly for different absorption coefficients of lamp plasma. It means that the absorption coefficient of lamp plasma has a great effect on the incident radiation in the photoreactor. This phenomenon can be explained from Eq. (3). With the increase of absorption coefficient, the diffusion coefficient of incident radiation decreases. Thus, more energy will be used to overcome the resistance of transfer inside the lamp and cannot be distributed into the space outside the lamp. As a result, the incident radiation both in the lamp and in the reaction space will become smaller. It means that the efficiency of energy decreases. Since the inactivation of microorganisms depends on the incident radiation, the inactivation of microorganisms must become slow and much more time is required for a safe inactivation of microorganisms. To obtain a high incident radiation in the UV reactor so as to save energy, an important step is to select UV lamp with low absorption coefficient on UV light.

### 4. Effect of Phase Function

The phase function determines the in-scattering from other directions. The value of  $C$  ranges from  $-1$  to  $1$ . A positive value indicates that more radiant energy is scattered forward than backward, and a negative value means that more radiant energy is scattered backward than forward; a zero value defines isotropic scattering (i.e., scattering that is equally in all directions). As shown in Eq. (3), the value of  $C$  can affect the value of the diffusion coefficient.

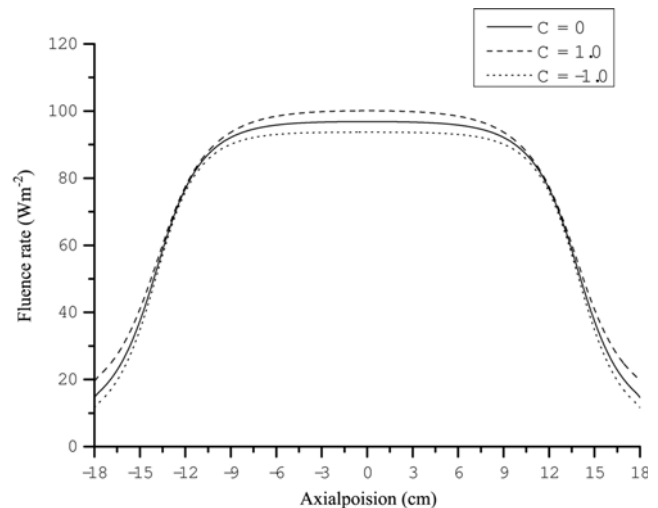


Fig. 6. The effect of phase function coefficient of the lamp plasma on incident radiation.

Fig. 6 shows the predicted incident radiation at the reactor outer wall with different values of phase function coefficient  $C$ . Although the prediction with  $C=0$  matches the experimental data much better, the phase function has only a small effect on the radiation distribution. It means that in the optimization, phase function can be regarded as an unimportant factor.

## CONCLUSIONS

The incident radiation in a photoreactor has been computed using an improved P-1 model and the finite volume method. The UV lamp is included in the computational domain and the multiple mediums in the photoreactor are considered. The boundary conditions of incident radiation at semi-transparent walls have been derived to link the P-1 equation in different mediums. The generation of UV light is described by an additional source term method. The present model does not require the results of analytical lamp emission model as the boundary conditions at the lamp surface and can be used to the photoreactor with multiple mediums.

The predicted incident radiation is verified with the experimental data in literature. Good agreement is obtained between the computed data and the experimental data. The effects of absorption coefficient, scattering coefficient and phase function of lamp plasma on the distribution of incident radiation have been discussed in detail. The most important factor affecting incident radiation in the reactor is the absorption coefficient of lamp plasma.

## REFERENCES

1. W. Hijnen, E. Beerendonk and G. J. Medema, *Water Res.*, **40**, 3 (2006).
2. S. M. Jacobm and J. S. Dranoff, *AIChE J.*, **16**, 359 (1970).
3. J. R. Bolton, *Water Res.*, **34**, 3315 (2000).
4. J. R. Bolton and M. I. Stefan, *Res. Chem. Intermed.*, **28**, 857 (2002).
5. D. Liu, J. Ducoste, S. Jin and K. Linden, *Journal of Water Supply: Research and Technology: AQUA*, **53**, 391 (2004).
6. E. R. Blatchley, *Water Res.*, **31**, 2205 (1997).

7. T. Akehata and T. Shirai, *J. Chem. Eng. Jpn.*, **5**, 385 (1972).
8. H. A. Irazoqui, J. Cerdíó and A. E. Cassano, *AIChE J.*, **19**, 460 (1973).
9. R. L. Romero, O. M. Alfano and A. E. Cassano, *Ind. Eng. Chem. Res.*, **36**, 3094 (1997).
10. O. M. Alfano, M. Vicente, S. Esplugas and A. E. Cassano, *Ind. Eng. Chem. Res.*, **29**, 1270 (1990).
11. Y. Quan, S. O. Pehkonen and B. Madhumita, *Ind. Eng. Chem. Res.*, **43**, 948 (2004).
12. S. Elyasi and F. Taghipour, *Chem. Eng. Sci.*, **65**, 5573 (2010).
13. G. Spadoni, E. Bandini and F. Santarelli, *Chem. Eng. Sci.*, **33**, 517 (1978).
14. Q. Yang, P. Ling Ang, M. B. Ray and S. O. Pehkonen, *Chem. Eng. Sci.*, **60**, 5255 (2005).
15. G. Raithby, *Numer. Heat Transfer, Part B: Fundamentals*, **36**, 241 (1999).
16. Q. Huang, T. Liu, J. Yang, L. Yao and L. Gao, *Chem. Eng. Sci.*, **66**, 3930 (2011).
17. V. K. Pareek and A. A. Adesina, *AIChE J.*, **50**, 1273 (2004).
18. B. Yu, B. Deng and C. N. Kim, *Chem. Eng. Sci.*, **63**, 5552 (2008).
19. J. E. Duran, F. Taghipour and M. Mohseni, *J. Photochem. Photobiol. A: Chemistry*, **215**, 81 (2010).
20. V. Pareek, S. Chong, M. Tadó and A. A. Adesina, *Asia-Pacific J. Chem. Eng.*, **3**, 171 (2008).